From *Proc. American Control Conference*, San Francisco, CA, June 1993.

Robust Nonlinear Control System Synthesis Method for Electro-Mechanical Pointing Systems with Flexible Modes

James H. Taylor and Jin Lu
Odyssey Research Associates
Ithaca, New York 14850-1326
email: jim@oracorp.com

Abstract [1]

This paper describes the design of a robust control system for a gun turret testbed called the ATB1000. The control system incorporates a control scheme based on sinusoidal-input describing function (SIDF) models of the testbed's drive subsystem to reduce the effects of backlash and nonlinear friction, and a dissipative control scheme to make the control system insensitive to the unmodeled dynamics and parameter imprecision associated with the flexible modes of the wheel/barrel subsystem.

1 Introduction

This paper describes the design of a robust control system for a gun turret testbed called the ATB1000 (see Fig. 1). This testbed is used to simulate the dynamics of a gun-firing platform and to test schemes for controlling and stabilizing the gun-firing process in the presence of uncertainties such as friction, backlash, flexible modes and gun recoil.

Our control objective is to obtain good transient response as the gun is slewed towards a specified reference angle and to maintain accurate pointing during gun firing. To achieve this, the controller must overcome the effects of gun recoil, nonlinear friction, and backlash. Furthermore, the control system is required to be robust to modeling uncertainties, such as parameter imprecision and unmodeled dynamics.

The testbed system can be decomposed into two subsystems which pose different control problems. The drive subsystem has limitations due to Coulomb friction and backlash, and the wheel/barrel subsystem has the "spill-over" problem associated with unmodeled high-frequency modes that occur in characterizing the motion of the flexible gun barrel. The control system described below incorporates a SIDF-based control scheme to reduce the effects of backlash and nonlinear friction, and a dissipative control scheme to make the control system insensitive to the unmodeled dynamics and parameter imprecision of the wheel/barrel subsystem.

This paper is organized as follows: In Section 2, we describe the testbed model and highlight some of the features of the system that make its control difficult; in Section 3, we formulate the control problem; in Sections 4 and 5 we detail the design of a robust control system for the testbed; finally, in Section 6, we verify the control system by simulating it on the testbed model.

[1] Support for the research described herein has been provided by the Defense Advanced Research Project Agency through the U.S. Army AMCCOM at Picatinny Arsenal, NJ by Contract Number DAAA21-92-C-0013.

2 Model Description

As shown in Fig. 1, the testbed consists of two subsystems:

- a drive subsystem, including a DC motor (with nonlinear friction), a gear chain (with backlash), and an elastic shaft;
- a wheel/barrel subsystem, including an inertia wheel (with nonlinear friction) and a flexible gun barrel.

In the work outlined below, we have neglected the effect of platform motion on the testbed.

2.1 The Drive Subsystem

The drive subsystem dynamics are governed by two sets of differential equations, depending on whether the gears are engaged on not. When the two gears are not engaged, there is no interaction between the DC motor and the elastic shaft:

$$J_m\ddot{\theta}_m = T_m - T_{mf} \quad (1)$$

$$J_b\ddot{\theta}_b = -T_s \quad (2)$$

where θ_m and θ_b are the angles of driving gear and driven gear, respectively. J_m, J_b are the inertia constants of the motor and elastic shaft assemblies, T_m is the torque of the motor, T_{mf} is the Coulomb friction torque on the motor

$$T_{mf} = b_m \operatorname{sgn}(\dot{\theta}_m)$$

where b_m is the magnitude of the friction torque and T_s is the reactive torque of the elastic shaft,

$$T_s = k_s(\theta_b - \theta_i) + b_s(\dot{\theta}_b - \dot{\theta}_i), \quad (3)$$

where k_s, b_s are spring and viscous friction constants respectively, and θ_i is the inertia wheel yaw angle.

When the two gears are engaged, the subsystem can be treated as if there were no gears. In this case, $\dot{\theta}_m = \dot{\theta}_b$ and $\theta_m = \theta_b + x_b$ (positive engagement) or $\theta_m = \theta_b$ (negative engagement), where x_b is the backlash gap. The differential equation governing the dynamics of θ_b is

$$(J_m + J_b)\ddot{\theta}_b = T_m - T_s - T_{mf} \quad (4)$$

We note that there is a "jump" in the states $\dot{\theta}_m$ and $\dot{\theta}_b$ at the moment the two gears become engaged. Let the moment of engagement be t_e, $\dot{\theta}_m(t_e^-)$ and $\dot{\theta}_b(t_e^-)$ the gear speeds before collision, $\dot{\theta}_m(t_e^+)$ and $\dot{\theta}_b(t_e^+)$ the gear speeds after collision. If we neglect the elasticity of the gear material, then by conservation of momentum we have:

$$\dot{\theta}_m(t_e^+) = \dot{\theta}_b(t_e^+) = \frac{J_m}{J_m + J_b}\dot{\theta}_m(t_e^-) + \frac{J_b}{J_m + J_b}\dot{\theta}_b(t_e^-) \quad (5)$$

The conditions for the gears to become engaged are:

1. (positive engagement)

$$\theta_m - \theta_b = x_b \text{ and } \dot{\theta}_m - \dot{\theta}_b > 0; \quad (6)$$

or

$$\theta_m - \theta_b = x_b \text{ and } \ddot{\theta}_m - \ddot{\theta}_b > 0; \quad (7)$$

2. (negative engagement)

$$\theta_m - \theta_b = 0 \text{ and } \dot{\theta}_m - \dot{\theta}_b < 0; \quad (8)$$

or

$$\theta_m - \theta_b = 0 \text{ and } \ddot{\theta}_m - \ddot{\theta}_b < 0; \quad (9)$$

We note that in the above conditions, the dynamics of θ_m and θ_b are governed by differential equations (1) and (2).

2.2 The Wheel/Barrel Subsystem

The gun barrel is a distributed parameter system which can be approximated by a lumped parameter system using the finite element method. After this approximation, the wheel/barrel subsystem is described by a state-space model of the following form:

$$\ddot{x} + D\dot{x} + Kx = B(T_s - T_g + T_{f_1} + T_{f_2}) \quad (10)$$

$$y = Cx \quad (11)$$

where $x \in \mathcal{R}^n$ is the subsystem state vector (vector of modal coordinates) and $y^T = [\theta_i \ \theta_{tip}]$ is the output vector; θ_i is the inertia wheel angle, and θ_{tip} is the gun barrel tip angle; matrices D, K, C and B are of appropriate dimensions. The arrays D and K are diagonal matrices with non-negative elements. T_g is the disturbance torque introduced by gun firing (recoil), and T_{f_1} and T_{f_2} are torques introduced by viscous and Coulomb friction between the inertia wheel and the supporting platform under it,

$$T_{f_1} = b_1\dot{\theta}_i \quad (12)$$

$$T_{f_2} = b_2 \ \mathrm{sgn}(\dot{\theta}_i) \quad (13)$$

where b_1 and b_2 are the friction coefficients.

The dimension of a flexible structure model are usually very high. From a numerical standpoint, we usually base the design of a controller for a flexible structure on a reduced-order model that contains the critical modes of the structure. In our case, we only consider four low-frequency modes of the wheel/barrel structure ($n = 4$ in (10)). One important issue is how to design a control based on the reduced-order model that does not destabilize the unmodeled modes when applied to the actual system.

3 Control Problem Statement

The objective of the control system is to smoothly slew and accurately point the gun barrel tip angle θ_{tip} with respect to a reference angle in the presence of gun firing, backlash, friction and unmodeled dynamics. To be specific, we want to find a control law $T_m = T_m(t)$ such that θ_{tip} will gracefully slew to θ_{ref} within some acceptable tolerance in reasonable time. To achieve this control objective, the control system must overcome the effect of backlash (the DC motor has no control over the wheel/barrel subsystem during disengagement) and Coulomb friction. In addition, the control system is required to be insensitive to modeling uncertainty, such as unmodeled high-frequency modes and system parameter imprecision of the flexible gun barrel.

Substituting (3) and (12) into (10) we can write the model of the wheel/barrel subsystem as

$$\ddot{x} + (D + (b_s + b_1)BC_1)\dot{x} + (K + k_sBC_1)x = Bu + Bw \quad (14)$$

where $\theta_i = C_1 x$, $u = b_s\dot{\theta}_b + k_s\theta_b$ and $w = T_g + T_{f_2}$.

The variable $u = b_s\dot{\theta}_b + k_s\theta_b$ can be considered as the input to system (14) and an output of the drive subsystem. Our approach to control design consists of two step: (1) find a control law u^d for the input u to system (14) such that the resulting θ_{tip} has the desired properties outlined above; (2) find a control law for T_m so that u as an output of the drive tracks the desired control law u^d found in step (1). This design approach is illustrated in Fig. 2, where controller $C_2(s)$ is designed in step (1) and controller C_{nl} is designed in step (2). In step (1), we will use a robust control scheme that does not destabilize unmodeled high-frequency modes and is insensitive to parameter uncertainty. In step (2), we will use a control scheme based on sinusoidal-input describing function (SIDF) models of the testbed's drive subsystem to deal with backlash and frictions. The SIDF models are used because we believe they provide the best characterization of the major nonlinear effects of the drive subsystem with which we are concerned: the sensitivity of the drive subsystem's input/output (I/O) behavior to the amplitude of the input signal due to backlash and friction.

4 Robust Control of the Wheel/Barrel Subsystem

Consider a constant feedback control law for system (14)

$$u = -F_1\dot{x} - F_2x \quad (15)$$

where F_1 and F_2 are two feedback gains.

Substituting (15) into (14) gives

$$\ddot{x} + (D + (b_s + b_1)BC_1 + BF_1)\dot{x} + (K + k_sBC_1 + BF_2)x = Bw \quad (16)$$

We note that $C_1 = [c_{11} \ \cdots \ c_{1i}]$ ($\theta_i = C_1x$) and $B = [b_1 \ \cdots \ b_n]^T$ in model (16) has the relation $c_{1i}b_i > 0, i = 1, \cdots, n$. In fact, the viscous bearing torque $T_{f_1} = b_1\dot{\theta}_i = b_1C_1\dot{x}$. If we assume that the wheel/barrel subsystem is only subject to the viscous bearing torque and has natural damping $D = 0$, then we have from (10),

$$\ddot{x} + Kx = -BT_{f_1} = -BC_1\dot{x} \quad (17)$$

We know that a system with only viscous bearing force (torque) is always energy dissipative. For system (17), this is true if and only if $c_{1i}b_i > 0, i = 1, \cdots, n$.

The following results give sufficient conditions for system (16) to be stable; refer to [1] for proofs:

Proposition 1: Assume diagonal matrices D and K satisfy $\dim(D) \geq n-1$ and $\dim(K) \geq (n-1)$. Then system (14) with control law (15) is asymptotically stable if $F_1 = f_1 C_1$ and $F_2 = f_2 C_1$ with $f_1 \geq 0$ and $f_2 \geq 0$ (namely, $u = f_1\dot{\theta}_i + f_2\theta_i$) •

In the following result, we neglect the damping in system (14), since a control law that stabilizes system (14) with zero natural damping is likely to stabilize the system with added non-zero natural damping.

Proposition 2: Let the damping matrix D in system (14) be zero, and the diagonal matrix K satisfy $\dim(K) \geq (n-1)$. System (14) with control law (15) is asymptotically stable if $F_1 = f_1 C_1 + f_3[1\ 0\ \cdots\ 0]$ and $F_2 = f_2 C_1$ with $f_1 \geq 0$, $f_2 \geq 0$ and $f_3 \geq 0$ (namely, $u = f_1\dot{\theta}_i + f_3\dot{x}_1 + f_2\theta_i$) •

Propositions 1 and 2 define control schemes that are robust with respect to system modeling errors and structural perturbations, because the control schemes do not depend on system parameters.

In the sequel, we will only consider the control scheme

$$u = f_1\dot{\theta}_i + f_3\dot{x}_1 + f_2\theta_i \tag{18}$$

where $f_i \geq 0, i = 1, 2, 3$. The freedom in choosing f_i's in the control scheme allows us to achieve other performance requirements such as desirable pole assignment while ensuring the stability of the system.

5 SIDF Control of the Drive Subsystem

Assume that we have found the control law for $u = b_s\dot{\theta}_b + k_s\theta_b$ for the wheel/barrel subsystem (14) which guarantees the required behavior of θ_{tip}. Now, we will design a nonlinear control based on sinusoidal-input describing function (SIDF) models of the drive subsystem such that $u = b_s\dot{\theta}_b + k_s\theta_b$ as an output of the drive subsystem matches this desired form (see Fig. 2). To generate a SIDF between input T_m and output $u = b_s\dot{\theta}_b + k_s\theta_b$, a sinusoidal function $T_m = a\sin(\omega t)$ is used as input to the drive subsystem. The corresponding output of the drive subsystem $u = b_s\dot{\theta}_b + k_s\theta_b$ is treated via Fourier analysis [3] to obtain the SIDF model $G(j\omega, a)$. For linear systems, such a model is independent of input amplitudes; in fact, it is the transfer function $G(j\omega)$. For nonlinear systems, however, SIDF models generally depend on the amplitude of the system input.

The procedure for designing a nonlinear controller using SIDF models for a number of input amplitudes is described in some detail in our companion paper [4], or in more depth in [3]. The end result of following that synthesis approach is a nonlinear control law in the following form:

$$T_m = f_P(e) + \int_0^t f_I(e)\,dt + \frac{d}{dt}f_D(e) \tag{19}$$

where T_m (the motor input) is the output of the controller, $e = \theta_{ref} - u$ with θ_{ref} an external input (see Fig. 2), and $f_P(\cdot)$, $f_P(\cdot)$ and $f_P(\cdot)$ are nonlinear functions obtained by an amplitude-desensitization process involving SIDF inversion. Again, for a detailed description of the SIDF-based control design method, see [3, 4].

6 Design and Simulation Study

The parameters of the testbed system are listed in Table 1. The dynamic response of θ_{tip} of the open-loop testbed system in the presence of initial non-zero condition ($\theta_{tip} \neq 0$), friction, backlash and gun-firing disturbance is shown in Fig. 3. From Fig. 3, we see that the modes of the barrel are quite lightly damped. We found that the damping ratio of the lowest-frequency mode is about 10%, and the damping ratios of other modes are less then 10%. Therefore, we use the degrees of freedon in (18) to increase the damping of the two lowest-frequency modes. Using any existing pole assignment methods (for example, see [2]) we find that when $u = -3.5\dot{x}_1 - 10\theta_i$, the damping factors of the first and second lowest-frequency modes are 40% and 20% respectively. By Proposition 2, the control scheme guarantees the stability of the system.

The SIDF-based control nonlinearities for the drive subsystem (19) is shown in Fig. 4. Figure 5 shows the uniformly fast response of $u = b_s\dot{\theta}_b + k_s\theta_b$ of the drive subsystem controlled by the nonlinear control to a step input v with different amplitudes. For comparison, Fig. 6 shows the response of $u = b_s\dot{\theta}_b + k_s\theta_b$ of the drive subsystem controlled by a linear control system (designed based on a linearized model of the testbed) to the step input v with different amplitudes. Fig. 6 also includes the response of $u = b_s\dot{\theta}_b + k_s\theta_b$ of the *linearized* model controlled by the linear control system. As mentioned earlier, the dynamic response of the SIDF-based nonlinear control system is insensitive to the amplitudes of input signal.

To summarize, the final composite nonlinear control law for the motor torque T_m is given by Eqn. (19) where $e = u^d - u = -3.5\dot{x}_1 - 10\theta_i - (b_s\dot{\theta}_b + k_s\theta_b)$ and $f_P(e), f_I(e), f_D(e)$ are the nonlinear functions shown in Fig. 4. The dynamic responses of θ_{tip} controlled by the nonlinear control law (19) is shown in Fig. 7, along with analogous results for inner-loop linear control. The closed-loop system is subject to several slew-angle commands (θ_{ref} values), as indicated; the responses are normalized by dividing by θ_{ref} so the amplitude sensitivity of the responses can be compared conveniently. The same levels of friction, backlash and gun-firing disturbance are used as in the open-loop case shown in Fig. 3. The closed-loop behavior of θ_{tip} has been improved greatly over the open-loop behavior.

A more detailed view of gun pointing accuracy is provided in Fig. 8, where the responses with linear and nonlinear control are shown for the smallest command $\theta_{ref} = 0.05$; note that the slowly decaying transients in the linear case completely dominate the response while the (much smaller) effect of gun-firing disturbance is seen in the nonlinear control case as being the dominant source of pointing error.

To test the robustness of this control scheme, we randomly

change the values of the components of vectors D, K, B and C_1 in system (14) without changing their signs. The closed-loop testbed system with control scheme (19) was always stable with such parameter changes and in most cases the dynamic response did not change noticeably.

7 Conclusion

We have developed a control system for the ATB1000 testbed model. The control system fulfilled our performance specification – it worked well in the presence of backlash, nonlinear friction, and gun-firing disturbances. The control system is robust with respect to both input amplitude and modeling uncertainties such as parameter imprecision and unmodeled dynamics of the flexible element.

References

[1] Jin Lu, "Robust Control of Semi-Rigid/Flexible Structures," *Proc. American Control Conference*, San Francisco, CA, 1993.

[2] G. Roppenecker and J. O'Reilly, "Parametric Output Feedback Controller Design," *Automatica, Vol. 25*, No. 2, pp. 259-265, 1989.

[3] Taylor, J. H., and K. L. Strobel, "Nonlinear Compensator Synthesis via Sinusoidal-Input Describing Functions," *Proc. American Control Conference*, Boston MA, pp. 1242-1247, 1985.

[4] Taylor, J. H., and J. Lu, "Computer-Aided Control Engineering Environment for the Synthesis of Nonlinear Control Systems," *Proc. American Control Conference*, San Francisco, CA, 1993.

notation	description	value	unit
x_b	backlash clearance	0-0.05	rad
b_s	spring viscosity	0.1	$Nm/rad\ sec^{-1}$
k_s	spring constant	34.3	Nm/rad
b_m	motor friction magnitude	0.5	1
J_m	motor and driving gear inertia	0.006	$Kg\ m^2$
J_b	driven gear and shaft inertia	0.01	$Kg\ m^2$
b_1	bearing viscosity	0.67	$Nm/rad\ sec^{-1}$
b_2	inertia wheel friction magnitude	0.1	1
D	damping matrix	diag([0 0.891 4.08 11.35])	$Nm/rad\ sec^{-1}$
K	stiffness matrix	diag([0 912.5 19124 148155])	Nm/rad
B^T	input gain vector	[5.7 27.6 -17.1 -14.9]	
C	output matrix	$\begin{bmatrix} 1.28 & 0.316 & -0.063 & -0.015 \\ 1.28 & -0.798 & -1.45 & 1.23 \end{bmatrix}$	

Table 1: Parameters of the ATB1000

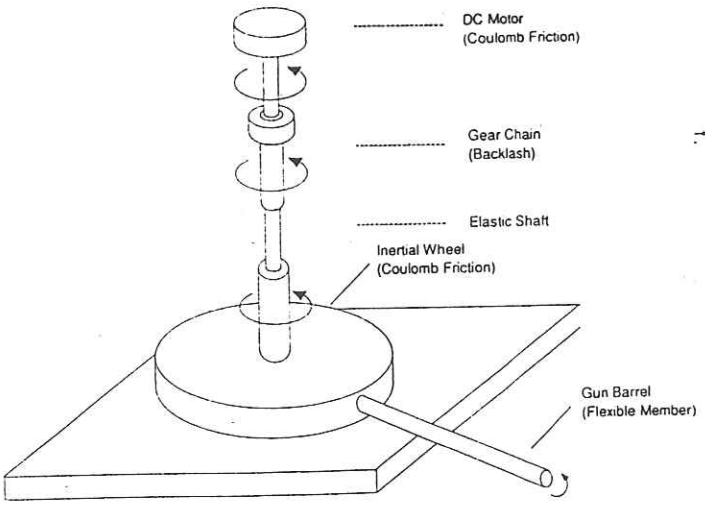

Fig. 1: A Schematic of a Tank Turret System

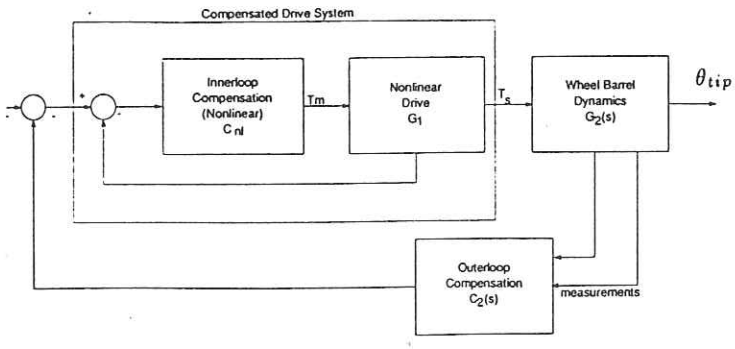

Fig. 2: Diagram of a Nonlinear Control System

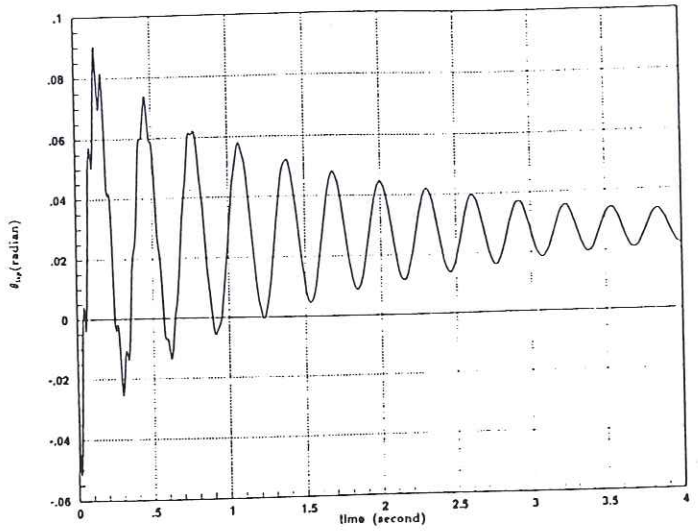

Fig. 3: Open-Loop Dynamic Response of θ_{tip}

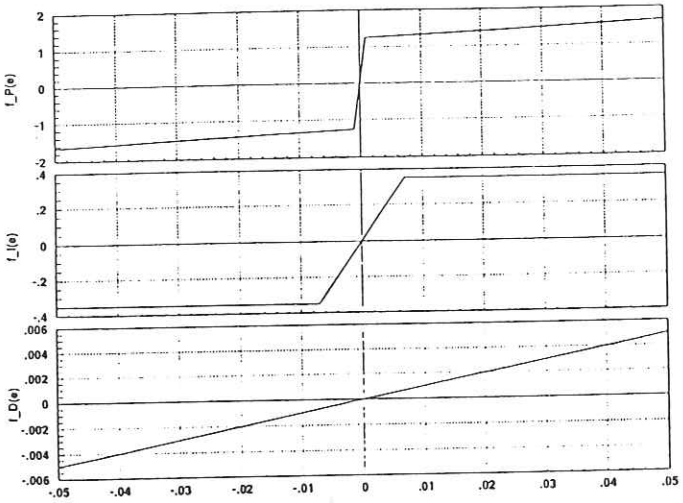

Fig. 4: Results of SIDF Inversion

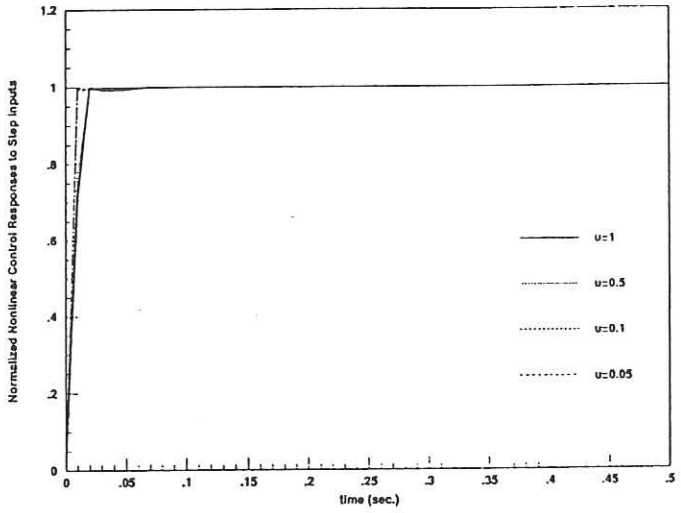

Fig. 5: Normalized Nonlinear Control Responses to Step Inputs u

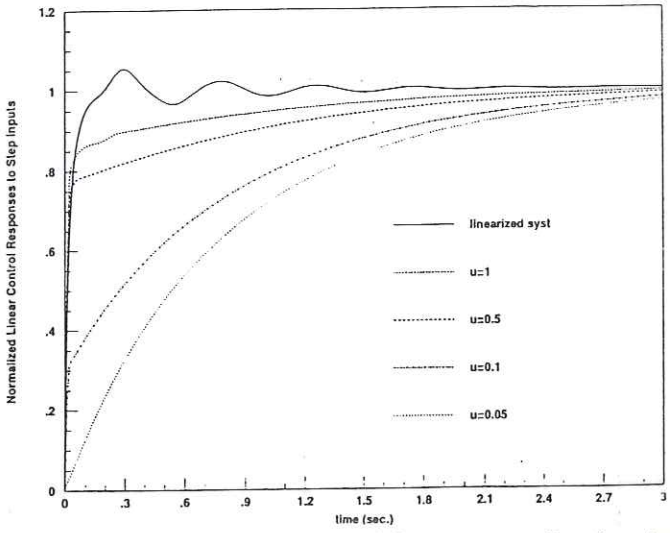

Fig. 6: Normalized Linear Control Responses to Step Inputs u

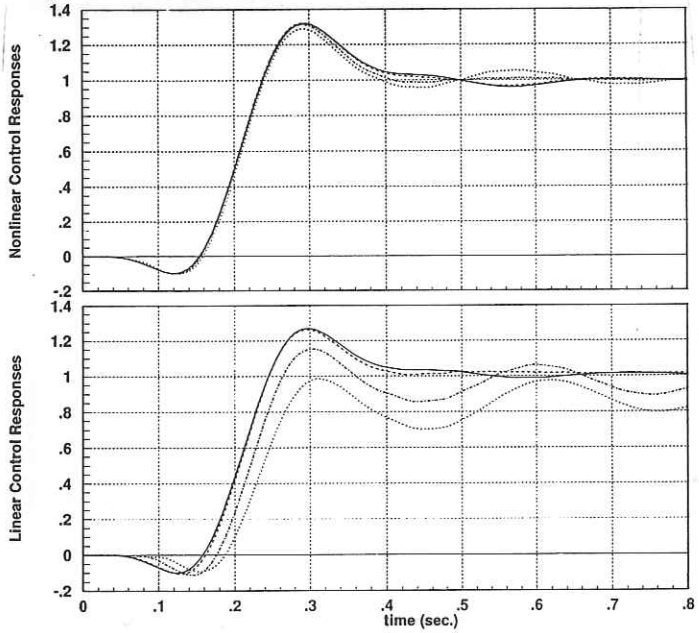

Fig. 7: Normalized Closed-Loop Responses of θ_{tip}

——: $\theta_{tip}^{ref} = 1(rad.)$, - - - : $\theta_{tip}^{ref} = .5(rad.)$,
- · - : $\theta_{tip}^{ref} = .1(rad.)$, · · · : $\theta_{tip}^{ref} = .05(rad.)$,

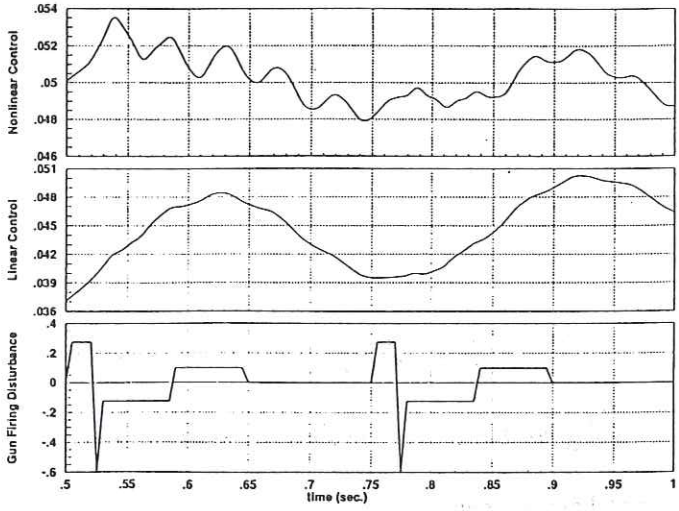

Fig. 8: Responses of θ_{tip} to Gun Firing Disturbance